

UC Irvine

UC Irvine Previously Published Works

Title

Tunable shrink-induced honeycomb microwell arrays for uniform embryoid bodies

Permalink

<https://escholarship.org/uc/item/5v87618g>

Journal

Lab on a Chip, 9(23)

ISSN

1473-0197

Authors

Nguyen, Diep
Sa, Silin
Pegan, Jonathan D
et al.

Publication Date

2009

DOI

10.1039/b914091c

Copyright Information

This work is made available under the terms of a Creative Commons Attribution License, available at <https://creativecommons.org/licenses/by/4.0/>

Peer reviewed

Tunable shrink-induced honeycomb microwell arrays for uniform embryoid bodies

Diep Nguyen,^a Silin Sa,^b Jonathan D. Pegan,^c Brent Rich,^c Guangxin Xiang,^b Kara E. McCloskey,^b Jennifer O. Manilay^d and Michelle Khine^{*a}

Received 14th July 2009, Accepted 18th September 2009

First published as an Advance Article on the web 12th October 2009

DOI: 10.1039/b914091c

Embryoid body (EB) formation closely recapitulates early embryonic development with respect to lineage commitment. Because it is greatly affected by cell-cell and cell-substrate interactions, the ability to control the initial number of cells in the aggregates and to provide an appropriate substrate are crucial parameters for uniform EB formation. Here we report of an ultra-rapid fabrication and culture method utilizing a laser-jet printer to generate closely arrayed honeycomb microwells of tunable sizes for the induction of uniform EBs from single cell suspension. By printing various microwell patterns onto pre-stressed polystyrene sheets, and through heat induced shrinking, high aspect micromolds are generated. Notably, we achieve rounded bottom polydimethylsiloxane (PDMS) wells not easily achievable with standard microfabrication methods, but critical to achieve spherical EBs. Furthermore, by simply controlling the size of the microwells and the concentration of the cell suspension we can control the initial size of the cell aggregate, thus influencing lineage commitment. In addition, these microwells are easily adaptable and scalable to most standard well plates and easily integrated into commercial liquid handling systems to provide an inexpensive and easy high throughput compound screening platform.

Introduction

The ability to recapitulate embryogenesis *in vitro* is a potentially powerful tool. For example, studying the effect of genetic mutations on developmental processes or screening small molecule libraries which direct stem cell differentiation can be highly informative in many fields such as developmental biology, drug discovery, and tissue engineering.^{1,2} When grown in suspension, under differentiating conditions, embryonic stem cells (ESCs) form three-dimensional aggregates known as embryoid bodies (EBs) comprised of cells from the three primary germ layers, *i.e.* endoderm, mesoderm, and ectoderm.^{2–10} Characteristic to EB differentiation is the progressive restriction of external signals and the increasing reliance on internal cell-cell signaling.² In addition, the transformation from ESCs to EBs is a highly conserved process as indicated by sequential gene expression corresponding to the initial formation of the primitive endoderm, followed by the formation of the primary germ layers leading to gastrulation and tissue level organization.^{11–13} In fact, studies have shown that the initial number of cells in the self-assembled aggregates highly influences the preferential commitment of the EB towards a specific germ layer.^{14,15} Thus the ability to control

the initial number of cells in an aggregate is critical for directed differentiation.

Currently the various methods for EB generation must strive to control size, morphology, uniformity and most importantly, reproducibility. To bridge the gap between academic research and industrial application a robust production method must be scalable as well. However, creating uniform EBs from murine embryonic stem cells (mESC) and human embryonic stem cells (hESC) has been a persistent challenge.^{14,16–18} In particular, traditional suspension culture has given rise to EB populations which are heterogeneous in size, morphology and thus epigenetic expression, rendering them unsuitable for potential clinical applications.^{2,19,20} This can be seen in previous studies indicating that suspension culture results in widely varied EB sizes (*e.g.* $\pm 60 \mu\text{m}$ for an EB of average diameter of $175 \mu\text{m}$).²¹ Further, compromise is often made between quantity and uniformity when choosing a culturing method. Such is the case with the widely used methylcellulose method which generates large numbers of EBs from single cells, but inherently results in asynchronous differentiation.^{22,23} Even in procedures such as the labor intensive hanging drop which can yield uniform EBs, the inherent limitation of culturing EBs in droplets less than $20 \mu\text{L}$ has made medium exchange and hence long term culture difficult.^{19,20,24,25,26}

Recently photolithographic microfabrication has enabled production of more uniform EBs arrays through cell patterning or geometric restrictions.²³ By using polydimethylsiloxane (PDMS) stencils and pyramidal wells, homogenous cell aggregates and EBs can be produced in large batch processes with the ease of medium exchange.^{16,27,28} The hydrophobic nature of PDMS has proven to help induce and maintain EBs in culture by minimizing cell adhesion. Recent studies show that providing

^aDepartment of Biomedical Engineering, University of California, Irvine, CA, USA. E-mail: mkhine@uci.edu

^bGraduate Group in Biological Engineering & Small-scale Technologies, University of California, Merced, USA. E-mail: kmccloskey@ucmerced.edu

^cSchool of Engineering, University of California, Merced, USA. E-mail: jpegan@ucmerced.edu

^dSchool of Natural Sciences, University of California, Merced, USA. E-mail: jmanilay@ucmerced.edu

a non-adherent, hydrophobic surface facilitates increased cell-cell interactions crucial for morphology and consequently genetic expression.^{15,29–34}

Most microfabrication approaches however, require complex steps, such as photolithography and anisotropic etching of silicon wafers, thus limiting their accessibility and adoption.^{20,35}

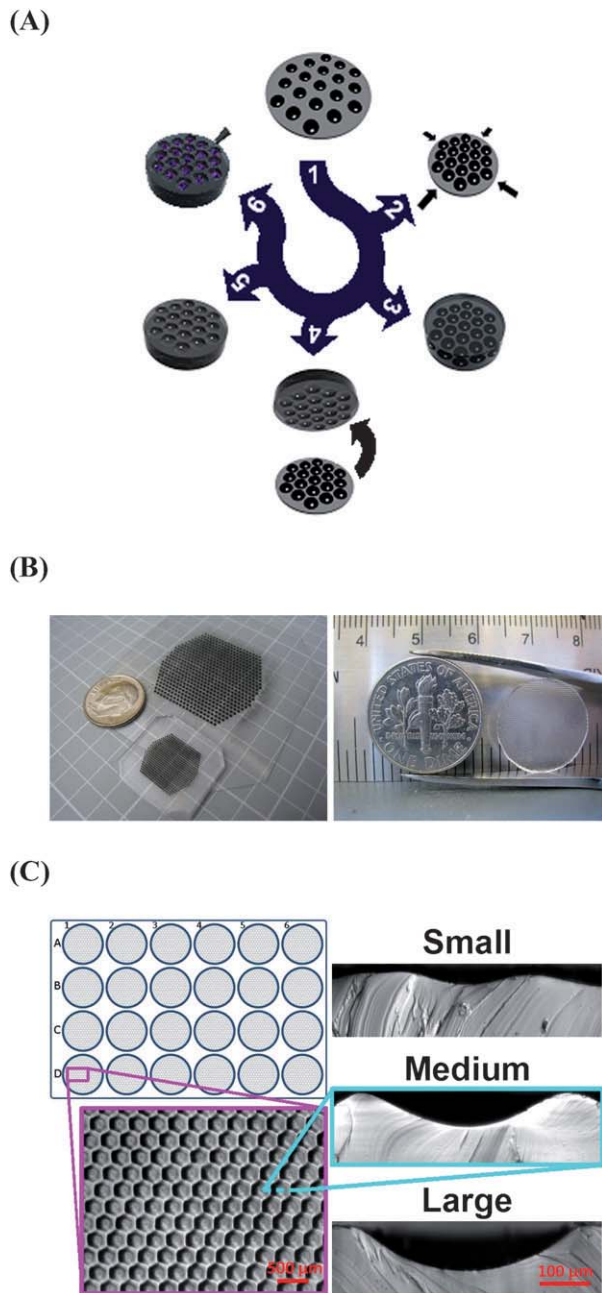


Fig. 1 Honeycomb microwell fabrication. (A) Microwell patterns of tunable sizes are printed on pre-stressed PS sheets (1) and are then heated to 155 °C (2) for approximately 5 minutes to form high-aspect micro-molds. PDMS is then molded (3) and removed (4) and cells are pipetted in (5). (B) PDMS molded onto the PS masters forming microwells. The bottom-side of the microwells are then bonded to glass slides (to prevent floating) and inserted into standard culture plates. (C) In addition the fabricated wells have tunable rounded bottoms which facilitate aggregation of single-cells; cross section of Small, Medium and Large wells.

Here we report an ultra-rapid fabrication method of closely arrayed microwells in a honeycomb configuration of customizable and well-controlled size (including diameter, depth and number of wells) negating the need for photolithography altogether. Notably, we achieve rounded bottom wells not easily achievable with standard microfabrication methods but critical to achieve spherical EBs.²¹ By printing various microwell patterns onto pre-stressed polystyrene (PS) sheets, and through heat induced shrinking, high aspect micromolds are generated with approximately 60% reduction in in-plane size.^{36–40} Polydimethylsiloxane (PDMS) is then molded onto the micromolds to form honeycomb microwells [Fig. 1]. The use of printable masters does not limit the fabrication of microwells to PDMS. Other polymeric substrates (*e.g.* polyethylene glycol (PEG) and agarose) can be likewise molded on the high aspect ratio molds *via* soft lithography as well.⁴¹ To control the number of cells per well, the cells are simply loaded into the wells by pipetting various concentrations of ESCs dissociated into single-cell suspensions.

Experimental

Fabrication of honeycomb microwells

Honeycomb microwell patterns were drafted in the drafting software AutoCAD (AutoDesk). In order to achieve a range of microwell diameters, accounting for the 60% reduction in size after shrinking of the pre-stressed PS sheet, we tested a range of varied drafting diameters: 250, 500, 750, and 890 μm . For ease of annotation, these correspond to final well sizes referenced as ‘Small’, ‘Medium’, ‘Large’ and ‘X-Large’. To minimize the spacing between wells, well patterns were placed in a staggered position as to minimize free surface area [Fig. 1a]. Next, well patterns were printed onto biaxially pre-stressed PS sheets (Grafix Inc.) using a laser-jet printer (Hewlett Packard 2600N). These PS molds were then heated to 155 °C for approximately 5 minutes to form high-aspect micro-molds.^{36–40} After molding with PDMS using standard procedures, the microwells, designed to fit in standard 24 well plates, are achieved. Notable, the shrinking process induces reflow of the toner ink to cause rounded bottoms as evidenced in the cross sections (Fig. 1c).

By repeated printing of the well patterns (by reinsertion into the laser-jet printer), the size and depth of the microwell patterns can be adjusted through the increase of ink deposition [Fig. 1b].

Notably, with increased number of prints, the wells grow both in diameter as well as depth [Fig 2a]. The fabrication of the honeycomb wells requires the heating of the PS sheets to 155 °C. Due to the difference in the shrinking temperature of the PS and that of toner melting temperature, which may vary slightly depending on the vendor, it is crucial that the devices be heated past the melting point of the toner to facilitate cohesive forces and the formation of well rounded wells. Next, to ensure the close packing of the microwells, the initial drafting patterns must be spaced such that upon heating will induce reflow of the ink without the merging of the ink droplets [Fig. 1a]. The close spacing minimizes the dead space between the wells and prevents the formation of non-uniform EBs on the outer perimeters due to

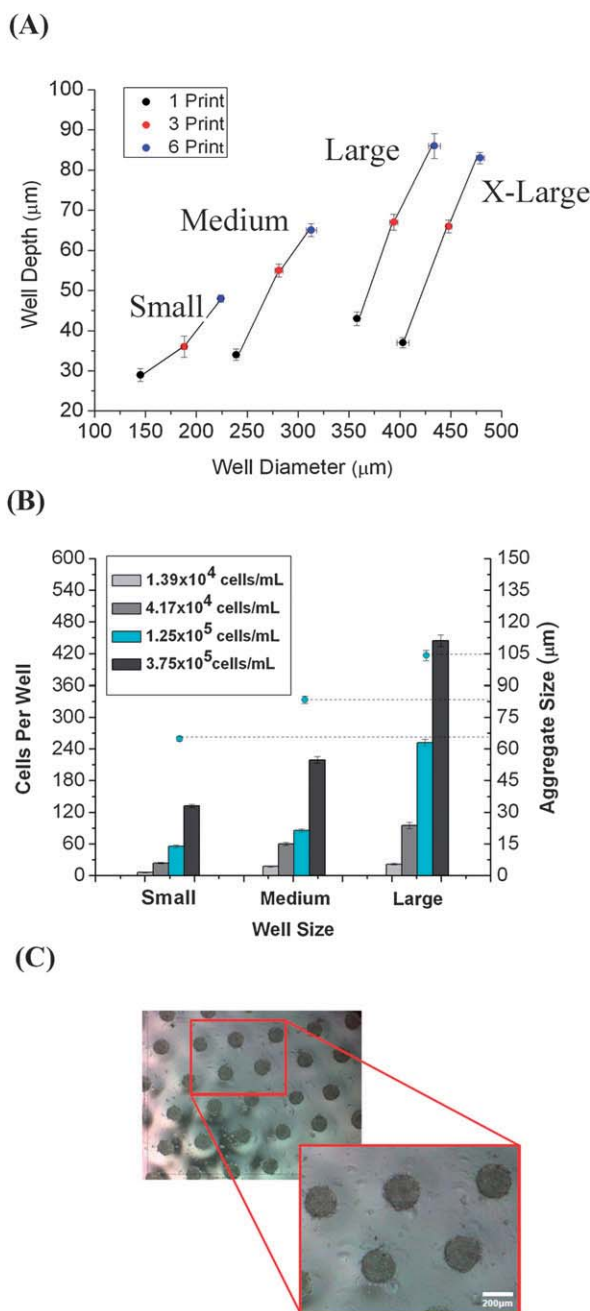


Fig. 2 Honeycomb microwell characterization. (A) Characteristic change of microwell diameters and depth with repeated prints for wells with drafting diameters of 250, 500, 750, and 890 μm . (B) Calibration of loading concentrations 1.39×10^4 cells/mL, 4.17×10^4 cells/mL, 1.25×10^5 cells/mL, and 3.75×10^5 cells/mL corresponding to Small, Medium and Large wells. Using the loading concentration of 1.25×10^5 cells/mL, aggregate sizes were characterized on day 2 for Small, Medium and Large wells. Standard error of mean was calculated for $N = 25$ per concentration and aggregate size, and $N = 10$ per depth and diameter measurement within the family curves. (C) Uniform aggregates from a higher seeding concentration of 3.75×10^5 cells/mL in large wells results in uniform EBs similar in size to the hanging drop method.

random clusters of ES cells. Once the device is made the toner will harden and the high-aspect micromolds can be used repeatedly to yield replicas of the same honeycomb wells.

With repeated printing we notice an increase in well dimensions. Notably, with increased number of prints, the wells grow both in diameter as well as depth [Fig 2a]. The variation in diameter, however, was seen to have a relatively constant increase of approximately 30 μm for all three drafting diameter with each successive printing. We have also noticed that the depth of the microwell is limited to the surface tension of the ink toner which is evident in the diminishing increase of aspect ratio beyond six repeated prints [Fig. 2a]. Thus we have seen that for all practical purpose of fabricating microwells with depths up to 100 μm , it is not necessary to exceed six repeated prints.

PDMS chemical treatment

To prevent the potential contamination of culture medium due to uncross-linked PDMS oligomers which may affect viability of mammalian cells, a modified method as reported by Millet *et al.* and Lee *et al.* was adopted to wash the PDMS.^{42,43} In this process PDMS honeycomb microwells were subjected to swelling and de-swelling through a continuous stirring in 1 L of solvent, with replacement of fresh solvent at indicated intervals. Briefly, the microwells were washed consecutively with pentane for 24 h; pentane 7 h; xylenes plus ethylbenzene 98.5% 1–2 h; xylenes 16 h; xylenes 7 h; EtOH 1–2 h; EtOH again for 16 h, and finally EtOH for 7 h (Sigma-Aldrich). Next the PDMS was rinsed with sterile DI water and dried at 70 $^{\circ}\text{C}$ overnight.

Cell culture

Mouse ES cells (mESC) (ATCC) and GFP-labeled myosin heavy chain mESC, courtesy of Conklin Lab, UC San Francisco, were maintained in Knock-out Dulbecco's modification of Eagle Medium (DMEM) (Gibco) supplemented with 15% Knock-out Serum Replacement (KSR) (Gibco), 100 $\mu\text{g/mL}$ penicillin-streptomycin (Invitrogen), 200 mM Glutamax (Invitrogen), 0.1 mM non-essential amino acids (NEAA) (Invitrogen), 0.1 mM β -mercaptoethanol (calbiochem) and 1000 U/mL leukemia inhibitory factor (LIF) (Chemicon) and plated on tissue cultured plates (Nunc) coated with 0.1% Gelatin (Sigma-Aldrich). To assure uniform distribution of cells during the loading process, ES cell colonies were dissociated into single cells. To this extent, cells washed twice with $1 \times$ phosphate buffered saline (PBS) (Gibco) and treated with TrypLE (Gibco) for 3 minutes. Next ES cells were gently dissociated using a P1000 pipette and spun down. ES cells were then re-suspended in EB medium, which has the same composition as ESC medium with the exclusion of LIF and KSR and supplemented with 15% fetal bovine serum (FBS).

Microwell loading

To load cells, the bottom of the microwells were bonded to single pieces of cover glass (Fisherbrand) using an O_2 plasma (SPI Supplies) and placed into each well of a standard 24-well plate containing 500 μL of EB medium. The initial 500 μL assisted in preventing air bubbles within the well and adhered the cover glass to the plate. Next an additional 1.0 mL of EB medium was placed into the well and was pipetted gently to remove any remaining air bubbles on the PDMS surface. ES cells were added at concentrations of 1.39×10^4 cells/mL, 4.17×10^4 cells/mL, 1.25×10^5 cells/mL, and 3.75×10^5 cells/mL [Fig 2b]. To achieve

uniform EB size requires the uniform distribution of single cells across the microwells, thus using a modified suspension culture method reported by Park *et al.* and Ungrin *et al.*, 1 mL of the ES cells were then gently pipetted with a P1000 and dispensed dropwise into each well of a 24-well plate.^{14,16} To prevent convective effects within each well of the 24-well plate which may disrupt the uniform distribution, ES cells were allowed to settle into the honeycomb microwells at room temperature for 15–30 minutes before being placed into the incubator.

To standardize the loading procedure, we have created a calibration curve which allows us to calculate the optimal cell density which prevents the formation of multiple EBs per well [Fig. 2b].

To show a direct correlation between tunable well size and EB size, aggregate sizes generated from a concentration of 1.25×10^5 cells/mL in Small, Medium and Large well were measured. We found that, for a given seeding concentration, the aggregate size varied linearly correlating to the original well size. Thus at 1.25×10^5 cells/mL, Small, Medium and Large wells yielded aggregates approximately 65, 85 and 105 μm in diameter, ± 5 , 8, and 11 μm respectively [Fig. 2b].

Next to determine the initial cell number attributed each microwell size, a custom software was used to count the number of cells distributed uniformly across each well size. Using a 1/3 dilution starting at 3.75×10^5 cells/mL to 1.39×10^4 cells/mL, we generated a family curve for Small, Medium and Large [Fig. 2b]. Notably, during the cell loading process, it was observed that the inherent non-restrictive geometry of the wells may induce the formation of multiple EBs per well at low loading densities. Due to the sparseness of the cell distribution, local colonies within a single microwell may not be able to adhere with one another, thus forming separate EBs. To solve this issue we have noted two possible solutions. First, we can either reduce the size of the microwell while maintaining the loading density constant, thus reducing the available well space to facilitate uniform aggregation. Second, we can increase the loading density of the cells while maintaining the well size constant, which will ensure the uniform coverage of the wells thus allowing all the single cells to aggregate into one single EB. At the concentration we used for our experiment, we observed 90% of the wells had single EB formation.

By using the calibration curve, we were also able to generate aggregates with initial cell numbers comparable to the hanging drop method, which uses approximately 500 cells/well, by seeding large wells at 3.75×10^5 cells/mL [Fig. 2b]. This resulted in the formation of uniform aggregates of approximately 200 μm in diameter [Fig. 2c]. Thus by varying the microwell size we are able to generate uniform aggregates of tunable sizes, with over 1,300 aggregates/cm² at the smallest size.

EB culture and flow cytometry

To observe the size dependent differentiation pattern, EB cultured in the Small, Medium, and Large microwells were transferred to a low adherent suspension culture dish (Corning) after two days.²¹ Oct-3/4 was used as an indicator of pluripotency (BD Biosciences).⁴⁴ In addition GATA4, Nestin, and CD-31, were used as indicators of early germ layer development (BD Biosciences). ES cells were stained for pluripotency before plating onto microwells. Two days after culture in microwells,

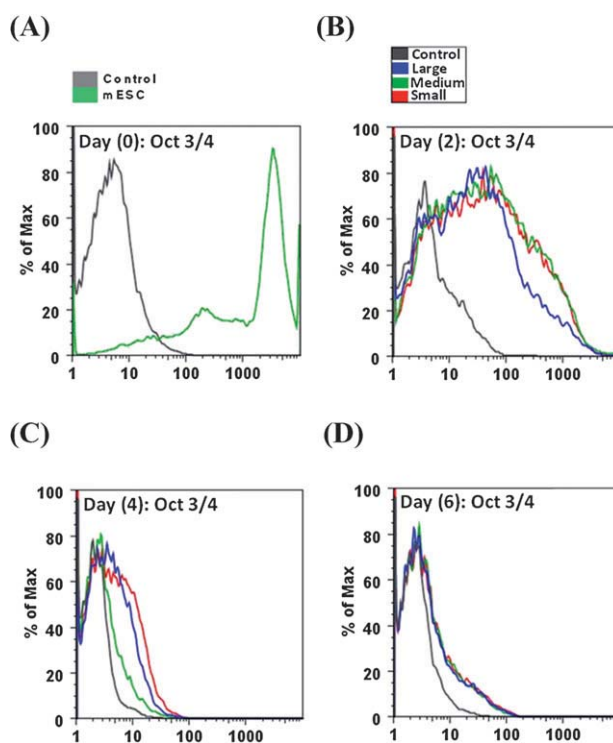


Fig. 3 EB differentiation occurs normally on chip as indicated by Oct-3/4 expression. Each separate sample of EBs derived from Small (Red), Medium (Green), and Large (Blue) wells corresponding to initial mESC aggregates of 130, 220, and 445 cells ± 15 , 30, and 56 cells respectively. (A) Day 0 mESC Oct-3/4 expression. (B) Oct-3/4 expression of EBs transferred on day 2. (C) Oct-3/4 expression of day 4 EBs, 2 days post transfer. (D) Oct-3/4 expression of day 6 EBs, 4 days post transfer. As control, all expressions are relative to unstained permeabilized cells.

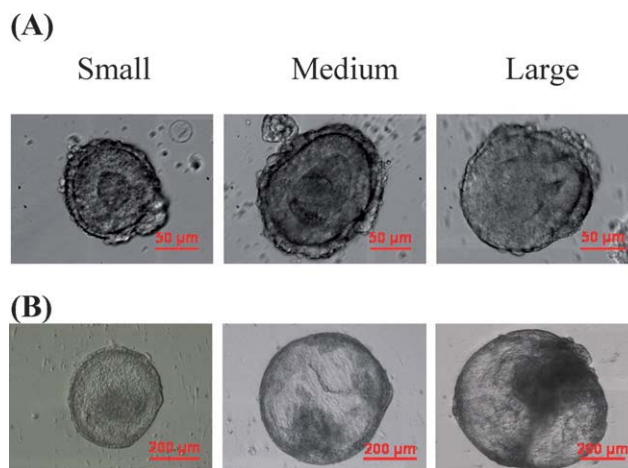
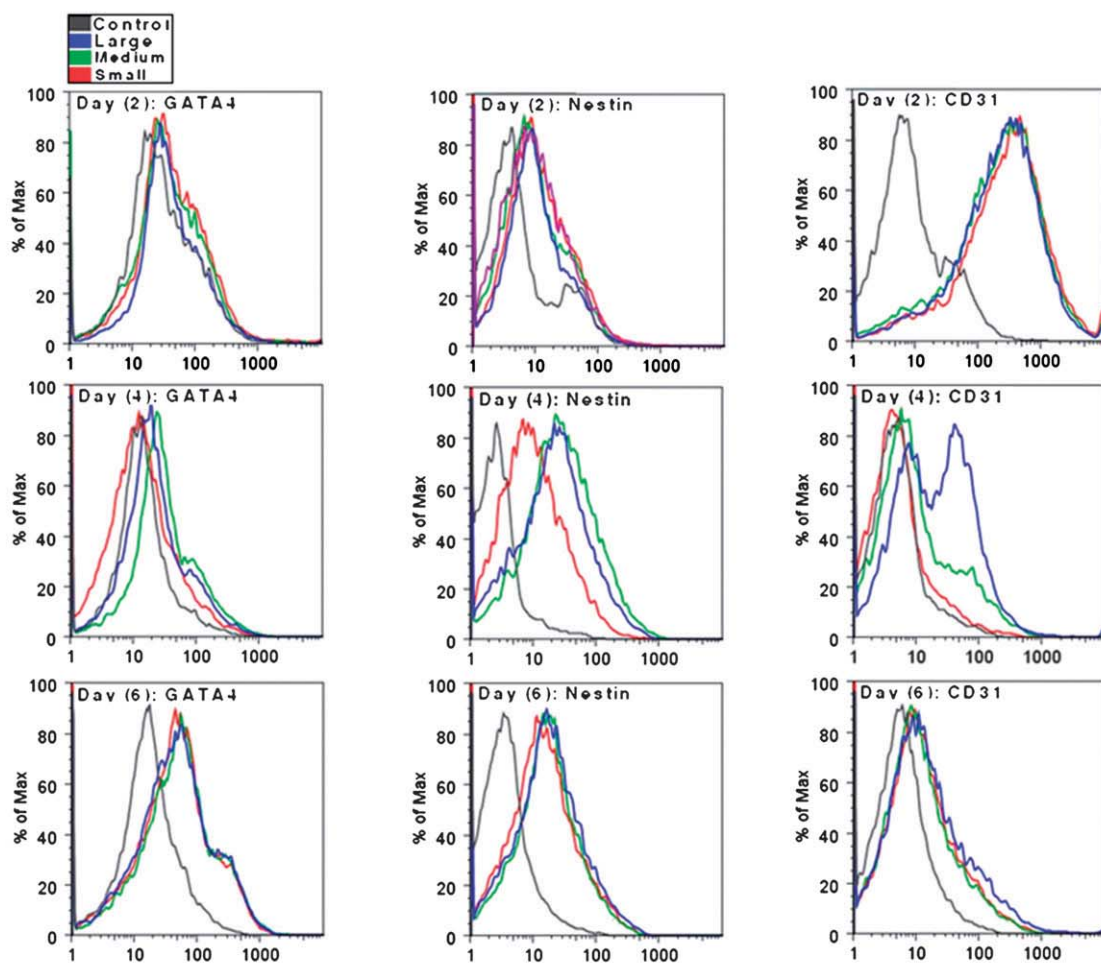


Fig. 4 EBs derived from microwells and transferred on day 2 to suspension culture plates. (A) Day 4 EBs in suspension of the 3 different sized wells show morphologically properly developing EBs. (B) Day 6 EBs in suspension develops cystic-like morphology.

uniform aggregates from each corresponding well size were transferred to suspension culture and samples were taken and stained for pluripotency as well as developmental markers. Subsequently EBs derived from the three well sizes were imaged and stained on day 4 and 6 for pluripotency and differentiation.

(A)



(B)

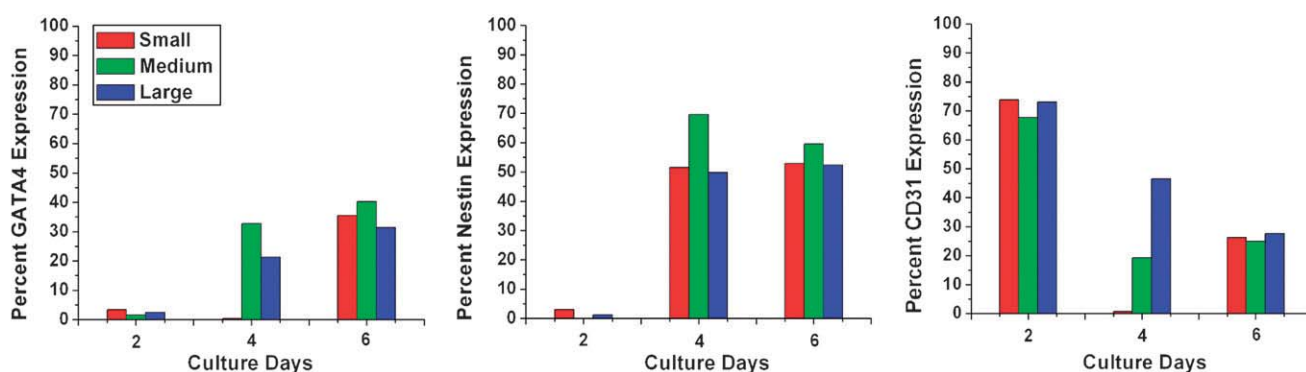


Fig. 5 EB Markers by FACS analysis. (A) Time course expression of GATA4, Nestin and CD-31 from EBs derived from Small (Red), Medium (Green) and Large (Blue) wells. GATA4 expression is upregulated by day 4 with medium-sized EB populations derived from initial aggregates of approximately 220 initial cells showing highest expression. GATA4 expression is upregulated in all populations by day 6. Nestin expression is upregulated by day 4, indicative of ectodermal layer. Small EBs populations derived from initial aggregates of approximately 130 cells show preferentially high expression of Nestin by day 4 relative to GATA4 and CD-31. By day 6, Nestin is uniformly upregulated in all three populations. CD-31 is detected in the starting mESC population as indicative of undifferentiated cells and is downregulated by day 4 in the small and medium populations more so than in the large EBs. By day 6 CD-31 is uniformly downregulated across all three populations. (B) The time course percent expression of GATA4, Nestin, and CD-31 for Small, Medium and Large microwells. All expression levels are relative to the control, unstained permeabilized cells.

Briefly, for Oct-3/4 staining EBs were dissociated into single cells and directly fixed with 4% formaldehyde (Gibco) and permeabilized with 0.7% Triton-X (mpbio) prior to staining. CD-31, GATA4 and Nestin were stained sequentially.

EB samples were dissociated into single cells and stained for CD-31 as an extracellular marker. Next, each sample was fixed with formaldehyde and permeabilized with Triton-X. GATA4 and Nestin were stained together as intracellular markers.

Results and discussion

EB formation and characterization

Critical for EB development is differentiation and eventual formation of the three primary germ layers. Thus to verify that uniform aggregates generated by the honeycomb microwells can develop into viable EBs, we tested for differentiation markers.

To accomplish this, Small, Medium and Large microwells, were seeded at the seeding density of 3.75×10^5 cells/mL. Assessment of differentiation characteristic between on chip and post transfer was correlated with the level of Oct-3/4 expression at different stages of EB differentiation relative to the initial ES population [Fig. 3]. As the aggregates develop into EBs by day 4 and 6 we continue to see a gradual decay of Oct-3/4. This can be correlated with the development of the three layers and subsequent formation of cystic EBs; this can be seen by morphology by day 4 and day 6 post transfer [Fig. 4].

To quantify the expression of the primary germ layers, flow cytometry (FACS ARIA) analysis was performed. For the formation of the endoderm and ectoderm layer we chose GATA4 and Nestin, respectively.^{45,46} These markers have been shown to be indicative of endoderm and ectoderm development and have been correlated with EB size.¹⁴ We also stained for CD-31 (also known as PCAM1). While CD-31 is an indicator of mesoderm development and early formation of endothelial progenitors, it has also shown to be expressed in ES cell populations and downregulated during the first three days of differentiation and subsequently upregulated by day 4 of EB formation.^{47,48}

As predicted, day 2 analysis indicates a lack of both GATA4 and Nestin in small, intermediate and large aggregate populations [Fig. 5a,b]. CD-31, however, which is expressed in pluripotent ES cells and gradually downregulated during the first three days of EB formation, is present in all three aggregate populations at day 2, indicating the initial stages of EB formation [Fig. 5c]. By day 4, both intermediate and large EB populations showed an upregulation of GATA 4 and Nestin [Fig. 5]. The EB population derived from the Small wells correlating to initial aggregates of approximately 130 cells [Fig. 2b], however, show a lack of both endoderm and mesoderm as indicated by the absence of GATA4 and CD-31. Previously, Park *et al.*, had reported that monolayers derived from EBs smaller than 100 μm and were then subjected to lineage specific differentiation, showed a preferentially higher ectoderm expression. Here we report that this observation is seen as early as day 4 of EB development as indicated by high Nestin expression relative to other markers [Fig. 5]. We also observe that the cells within the largest EB aggregates showed a preferentially higher retained expression of CD-31 relative to the small and intermediate EB populations by day 4.

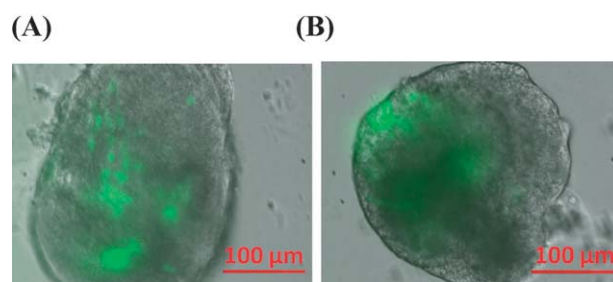


Fig. 6 Beating EBs derived from microwells. (A) EBs derived from large wells seeded at density of 3.75×10^5 cells/mL develops into beating cardiomyocyte by day 14 as detected by GFP-labeled myosin heavy chain reporter gene. EBs were transferred from suspension culture onto gelatin coated culture plates at day 2. (B) Beating EBs derived from the traditional hanging drop method shows similar GFP expression.

By day 6, we have noticed that all three EB populations have expressed uniform levels of GATA4, Nestin, and CD-31 [Fig. 5]. We have also observed that by day 6, all EB populations seem to appear to have developed the characteristic cystic center based on morphology, however, also retain a slight size difference [Fig. 4b]. This leads us to believe that the preferential bias in lineage specification previously reported occurs during the EB formation.¹⁴ Thus, based on our analysis, and data previously reported, we believe that the tunable geometry in addition to the simple fabrication method, honeycomb microwells can be used as a possible method for the enrichment of lineage-specific tissue derivation. Further, by exploiting the preferential differences in lineage commitment, seen as early as day 4, EBs derived from microwells may be selected for further directed differentiation.

Lastly, to show that EBs derived from microwells are healthy and can develop into functional tissue level organization we compared the ability of EBs derived from microwells and those from the traditional hanging drop method to form beating cardiomyocytes. To accomplish this, large wells seeded at 3.75×10^5 cells/mL were induced to form beating cardiomyocytes by transferring the EB colonies from suspension culture to gelatin coated culture plates after two days. Using a GFP labeled myosin heavy chain reporter gene as an indicator of cardiac tissue, fluorescence imaging was taken of the beating colonies [Fig. 6]. We observed that EBs derived from microwells were able to develop into beating cardiomyocytes by day 14 [Fig. 6a]. In addition the GFP expression from populations derived from microwells [Fig. 6a] were similar to those derived from the traditional hanging drop method [Fig. 6b] (data not shown). Thus we conclude that EBs derived from honeycomb microwell exhibit normal differentiation patterns. Furthermore, they are able to form functional tissue level organization comparable to traditional method.

Conclusions

We report a novel method for the fabrication of honeycomb microwells utilizing a laser-jet printer and replica molding. In addition we have shown functional application of the devices for the induction of uniform EBs of tunable sizes. By printing microwell patterns onto biaxially-stressed PS sheets and through heat induced shrinking, high aspect micromolds are generated. By molding PDMS onto the PS masters, honeycomb-shaped

microwells are formed. In addition, through the inherent fabrication method, we are able to generate rounded bottom wells which facilitate the formation of spherical EBs and which are potentially much less restrictive to diffusive transport. By varying the size of the honeycomb wells, we are able to control the initial number of cell aggregates thus enabling control of the rate of EB growth and differentiation, which has been shown to affect lineage commitment. Notably, honeycomb microwells can be integrated into standard cell culture plates providing a low-cost, robust method of high-throughput EB culture applicable in both academic and industrial settings. Additionally, with the application of Rho-associated kinase (ROCK) inhibitors, which permits the single cell dissociation of hESCs, this approach is also extensive to hESCs and induced pluripotent stem (iPS) cells.^{49–51} As such, this technology is a useful tool for a large range of applications.

Acknowledgements

We would like to thank Dr. Bruce Conklin and the Conklin lab, particularly Jason Park and Kenta Nakamura for providing us with mESCs. This project was funded by the California Institute of Regenerative Medicine (CIRM) and Shrink Nanotechnologies Inc.

References

- 1 A. Mehta, V. B. Konala, A. Khanna and A. S. Majumdar, *Cell Biol. Int.*, 2008, **32**, 1412–1424.
- 2 A. M. Bratt-Leal, R. L. Carpenedo and T. C. McDevitt, *Biotechnol. Prog.*, 2009, **25**, 43–51.
- 3 S. C. Zhang, M. Wernig, I. D. Duncan, O. Brustle and J. A. Thomson, *Nat. Biotechnol.*, 2001, **19**, 1129–1133.
- 4 G. Yirme, M. Amit, I. Laevsky, S. Osenberg and J. Itskovitz-Eldor, *Stem Cells Dev.*, 2008, **17**, 1227–1241.
- 5 M. Schuldiner, R. Eiges, A. Eden, O. Yanuka, J. Itskovitz-Eldor, R. S. Goldstein and N. Benvenisty, *Brain Res.*, 2001, **913**, 201–205.
- 6 E. Sachlos and D. T. Auguste, *Biomaterials*, 2008, **29**, 4471–4480.
- 7 B. E. Reubinoff, P. Itsykson, T. Turetsky, M. F. Pera, E. Reinhartz, A. Itzik and T. Ben-Hur, *Nat. Biotechnol.*, 2001, **19**, 1134–1140.
- 8 S. Nishikawa, S. Nishikawa, M. Hirashima, N. Matsuyoshi and H. Kodama, *Development*, 1998, **125**, 1747–1757.
- 9 D. S. Kaufman, E. T. Hanson, R. L. Lewis, R. Auerbach and J. A. Thomson, *Proc. Natl. Acad. Sci. U. S. A.*, 2001, **98**, 10716–10721.
- 10 A. Bigas, D. I. Martin and I. D. Bernstein, *Blood*, 1995, **85**, 3127–3133.
- 11 A. Mogi, H. Ichikawa, C. Matsumoto, T. Hieda, D. Tomotsune, S. Sakaki, S. Yamada and K. Sasaki, *Tissue Cell*, 2009, **41**, 79–84.
- 12 J. Itskovitz-Eldor, M. Schuldiner, D. Karsenti, A. Eden, O. Yanuka, M. Amit, H. Soreq and N. Benvenisty, *Mol. Med.*, 2000, **6**, 88–95.
- 13 T. Dvash, Y. Mayshar, D. Barker, O. Yanuka, K. J. Kotkow, L. L. Rubin, N. Benvenisty and R. Eiges, *Hum. Reprod.*, 2004, **19**, 2875–2883.
- 14 J. Park, C. H. Cho, N. Parashurama, Y. W. Li, F. Berthiaume, M. Toner, A. W. Tilles and M. L. Yarmush, *Lab Chip*, 2007, **7**, 1018–1028.
- 15 D. Falconnet, G. Csucs, H. M. Grandin and M. Textor, *Biomaterials*, 2006, **27**, 3044–3063.
- 16 M. D. Ungrin, C. Joshi, A. Nica, C. Bauwens and P. W. Zandstra, *PLoS One*, 2008, **3**, e1565.
- 17 J. M. Karp, J. Yeh, G. Eng, J. Fukuda, J. Blumling, K. Y. Suh, J. Cheng, A. Mahdavi, J. Borenstein, R. Langer and A. Khademhosseini, *Lab Chip*, 2007, **7**, 786–794.
- 18 S. M. Dang, S. Gerecht-Nir, J. Chen, J. Itskovitz-Eldor and P. W. Zandstra, *Stem Cells*, 2004, **22**, 275–282.
- 19 W. G. Lee, D. Ortmann, M. J. Hancock, H. Bae and A. Khademhosseini, *Tissue Eng. Part C Methods*, 2009, DOI: 10.1089/ten.tec.2009.0248.
- 20 S. M. Dang, M. Kyba, R. Perlingeiro, G. Q. Daley and P. W. Zandstra, *Biotechnol. Bioeng.*, 2002, **78**, 442–453.
- 21 J. M. Karp, J. Yeh, G. Eng, J. Fukuda, J. Blumling, K. Y. Suh, J. Cheng, A. Mahdavi, J. Borenstein, R. Langer and A. Khademhosseini, *Lab Chip*, 2007, **7**, 786–794.
- 22 H. Kurosawa, *J. Biosci. Bioeng.*, 2007, **103**, 389–398.
- 23 H. Liu, S. F. Collins and L. J. Suggs, *Biomaterials*, 2006, **27**, 6004–6014.
- 24 E. S. Ng, R. P. Davis, L. Azzola, E. G. Stanley and A. G. Elefanty, *Blood*, 2005, **106**, 1601–1603.
- 25 G. M. Keller, *Curr. Opin. Cell Biol.*, 1995, **7**, 862–869.
- 26 T. Yamada, M. Yoshikawa, S. Kanda, Y. Kato, Y. Nakajima, S. Ishizaka and Y. Tsunoda, *Stem Cells*, 2002, **20**, 146–154.
- 27 N. Yazdi and K. Najafi, *J. Microelectromech. Syst.*, 2000, **9**, 544–550.
- 28 H. C. Moeller, M. K. Mian, S. Shrivastava, B. G. Chung and A. Khademhosseini, *Biomaterials*, 2008, **29**, 752–763.
- 29 B. Valamehr, S. J. Jonas, J. Polleux, R. Qiao, S. Guo, E. H. Gschwend, B. Stiles, K. Kam, T. J. Luo, O. N. Witte, X. Liu, B. Dunn and H. Wu, *Proc. Natl. Acad. Sci. U. S. A.*, 2008, **105**, 14459–14464.
- 30 B. Hinz, G. Celetta, J. J. Tomasek, G. Gabbiani and C. Chaponnier, *Mol. Biol. Cell*, 2001, **12**, 2730–2741.
- 31 A. Folch, B. H. Jo, O. Hurtado, D. J. Beebe and M. Toner, *J. Biomed. Mater. Res.*, 2000, **52**, 346–353.
- 32 A. J. Engler, H. L. Sweeney, D. E. Discher and J. E. Schwarzbauer, *J. Musculoskelet. Neuronal Interact.*, 2007, **7**, 335.
- 33 A. J. Engler, S. Sen, H. L. Sweeney and D. E. Discher, *Cell*, 2006, **126**, 677–689.
- 34 J. Elisseeff, A. Ferran, S. Hwang, S. Varghese and Z. Zhang, *Stem Cells Dev.*, 2006, **15**, 295–303.
- 35 J. C. Mohr, J. J. de Pablo and S. P. Palecek, *Biomaterials*, 2006, **27**, 6032–6042.
- 36 C. S. Chen, J. Pegan, J. Luna, B. Xia, K. McCloskey, W. C. Chin and M. Khine, *J. Visualized Exp.*, 2008, DOI: 10.3791/692.
- 37 C. S. Chen, D. N. Breslauer, J. I. Luna, A. Grimes, W. C. Chin, L. P. Lee and M. Khine, *Lab Chip*, 2008, **8**, 622–624.
- 38 A. Grimes, D. N. Breslauer, M. Long, J. Pegan, L. P. Lee and M. Khine, *Lab Chip*, 2008, **8**, 170–172.
- 39 C. C. Fu, A. Grimes, M. Long, C. G. L. Ferri, B. D. Rich, S. Ghosh, S. Ghosh, L. P. Lee, A. Gopinathan and M. Khine, *Adv. Mater.*, 2009, DOI: 10.1002/adma.200902294.
- 40 M. Long, M. A. Sprague, A. A. Grimes, B. D. Rich and M. Khine, *Appl. Phys. Lett.*, 2009, **94**, 133501.
- 41 Y. Ling, J. Rubin, Y. Deng, C. Huang, U. Demirci, J. M. Karp and A. Khademhosseini, *Lab Chip*, 2007, **7**, 756–762.
- 42 L. J. Millet, M. E. Stewart, J. V. Sweedler, R. G. Nuzzo and M. U. Gillette, *Lab Chip*, 2007, **7**, 987–994.
- 43 J. N. Lee, C. Park and G. M. Whitesides, *Anal. Chem.*, 2003, **75**, 6544–6554.
- 44 S. M. Mitalipov, H. C. Kuo, J. D. Hennebold and D. P. Wolf, *Biol. Reprod.*, 2003, **69**, 1785–1792.
- 45 C. Wiese, A. Rolletschek, G. Kania, P. Blyszczuk, K. V. Tarasov, Y. Tarasova, R. P. Wersto, K. R. Boheler and A. M. Wobus, *Cell. Mol. Life Sci.*, 2004, **61**, 2510–2522.
- 46 R. J. Arceci, A. A. King, M. C. Simon, S. H. Orkin and D. B. Wilson, *Mol. Cell. Biol.*, 1993, **13**, 2235–2246.
- 47 D. Vittet, M. H. Prandini, R. Berthier, A. Schweitzer, H. Martin-Sisteron, G. Uzan and E. Dejana, *Blood*, 1996, **88**, 3424–3431.
- 48 H. M. DeLisser, P. J. Newman and S. M. Albelda, *Immunol. Today*, 1994, **15**, 490–495.
- 49 K. Watanabe, M. Ueno, D. Kamiya, A. Nishiyama, M. Matsumura, T. Wataya, J. B. Takahashi, S. Nishikawa, S. Nishikawa, K. Muguruma and Y. Sasai, *Nat. Biotechnol.*, 2007, **25**, 681–686.
- 50 T. Ishizaki, M. Uehata, I. Tamechika, J. Keel, K. Nonomura, M. Maekawa and S. Narumiya, *Mol. Pharmacol.*, 2000, **57**, 976–983.
- 51 D. A. Claassen, M. M. Desler and A. Rizzino, *Mol. Reprod. Dev.*, 2009, **76**, 722–732.